Vaccine: X 20 (2024) 100559

Contents lists available at ScienceDirect

Vaccine: X

journal homepage: www.elsevier.com/locate/jvacx

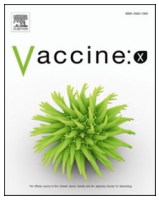

Enhanced production of recombinant coxsackievirus A16 using a serum-free HEK293A suspension culture system for bivalent enterovirus vaccine development

Yi-An Chen [a,b], Yu-Sheng Shen [b], Chih-Yeu Fang [b], Ting-Ting Chan [c], Shang-Rung Wu [c], Jen-Ren Wang [d,e], Suh-Chin Wu [a], Chia-Chyi Liu [b,*]

[a] Institute of Biotechnology, National Tsing Hua University, Hsinchu, Taiwan
[b] National Institute of Infectious Diseases and Vaccinology, National Health Research Institutes, Zhunan Town, Miaoli County, Taiwan
[c] School of Dentistry & Institute of Oral Medicine, National Cheng Kung University, Tainan, Taiwan
[d] Department of Medical Laboratory Science and Biotechnology, National Cheng Kung University, Tainan, Taiwan
[e] National Institute of Infectious Diseases and Vaccinology, National Health Research Institutes, Tainan, Taiwan

ARTICLE INFO

Keywords:
Coxsackievirus A16 (CVA16)
Hand, foot, and mouth disease (HFMD)
DNA-launched infectious clone
Inactivated whole virion vaccine
Serum-free HEK293A suspension culture
Bivalent vaccine

ABSTRACT

Coxsackievirus A16 (CVA16) is one of the primary pathogens that causes hand, foot, and mouth disease (HFMD) in young children. In previous studies, CVA16 vaccine development has encountered several challenges, such as inefficient replication of the CVA16 virus in present culture systems, the induction of only mild neutralizing antibody titers, and neutralizing antibodies induced by certain vaccine candidates that are unable to protect against CVA16 viral challenge. In this study, we constructed a DNA-launched CVA16 infectious clone (CVA16ic) based on the genomic sequence of the CVA16 N5079 strain to minimize interference from viral quasispecies. The biochemical properties of this CVA16ic strain were similar to those of its parental strain. Serum-free HEK293A suspension cells, which produced higher virus titers than Vero cells, were demonstrated to improve CVA16 production yields. In addition, our study showed that inactivated EV-A71 antigens could enhance the immunogenicity of inactivated CVA16 mature/full particles (F-particles), suggesting that a bivalent CVA16 and EV-A71 vaccine may be an effective strategy for CVA16 vaccine development. These findings are expected to provide novel strategies and accelerate the development of bivalent HFMD vaccines.

Introduction

Coxsackievirus A16 (CVA16), a member of the *Enterovirus* genus, is one of the primary pathogens responsible for causing hand, foot, and mouth disease (HFMD) in children. CVA16 was first isolated in 1951 and has been associated with numerous outbreaks worldwide, particularly in Asia-Pacific regions [1–4]. Although CVA16 infection typically manifests as mild clinical symptoms, it can sometimes lead to severe complications such as encephalitis and acute flaccid paralysis. Cocirculation of CVA16 with other enterovirus serotypes, such as enterovirus A71 (EV-A71), raises concerns about genetic recombination and complicates the clinical management of HFMD. With the successful development of inactivated EV-A71 vaccines, attention has turned toward the development of CVA16 vaccines [3,4].

The efficacy of CVA16 vaccines utilizing different platforms, including live-attenuated, inactivated, and virus-like particles, has been preliminarily evaluated in several animal studies over the past few decades [5–11]. Currently, only a few CVA16 vaccine candidates are undergoing clinical trial evaluation, including monovalent CVA16 vaccines and bivalent CVA16/EV-A71 vaccine designs (ClinicalTrials.gov identifiers: NCT04182932, NCT04637919 and NCT06063057). Previous studies have highlighted some challenges encountered in CVA16 vaccine development, such as inefficient replication of the CVA16 virus in the currently available culture system, the induction of only mild neutralizing antibody titers, and neutralizing antibodies induced by certain vaccine candidates that were unable to protect against viral challenge with the CVA16 virus [5,12,13]. These challenges have contributed to the prolonged progression of CVA16 vaccine

* Corresponding author at: Vaccine R&D Center, National Institute of Infectious Diseases and Vaccinology, National Health Research Institutes, Zhunan Town, Miaoli County 35053, Taiwan.
E-mail address: 010113@nhri.edu.tw (C.-C. Liu).

https://doi.org/10.1016/j.jvacx.2024.100559
Received 31 May 2024; Received in revised form 4 September 2024; Accepted 17 September 2024
Available online 19 September 2024

development, underscoring the importance of further novel approaches to address these challenges. Additionally, these novel approaches must consider adhering to PIC/S GMP quality standards for virus production.

In past studies, the Vero and KMB17 cell lines have been used for the production of inactivated CVA16 vaccine candidates [5,8]. However, these cell lines are adherent cells, and scaling up their production using microcarriers in bioreactor or cell factory presents additional costs for vaccine development and production. Each amplification process requires a dissociation/reattachment step, which poses a risk of possible contamination during cell passage operations. In addition, the viral yields of CVA16 were significantly lower than those of EV-A71 in these cell lines. Recently, a serum-free HEK293A suspension culture process was developed to improve coxsackievirus A10 yields [14]. This new technique reduces the use of additional chemical reagents and avoids the disadvantages of cell aggregation that might occur during the dissociation/reattachment step.

Infectious clones, DNA plasmids containing full viral genomes, can generate live viruses via the delivery of DNA or mRNA into a suitable cell line. The reverse genetics technique is a powerful tool in virology, enabling the study of viral replication, pathogenesis, and virus-host cell interactions by offering precise control of the viral genome. Moreover, infectious clones play a pivotal role in viral vaccine development [4,15–18]. In the manufacturing of inactivated influenza vaccines, the HA and NA glycoproteins are substituted with desired sequences in a high-growth influenza virus infectious clone to ensure a higher production yield [19]. Currently, several CVA16 infectious clones have been reported, and most of them require laborious *in vitro* RNA synthesis steps for each batch of viruses [20–25].

Multivalent vaccines represent a well-established strategy of combining individual vaccines into a single formulation to provide protection against multiple pathogens. The advantages of multivalent vaccines include simplifying the immunization process and reducing the expenses associated with vaccine delivery, storage requirements, and personnel [26]. The administration of multivalent vaccines, including the measles/mumps/rubella (MMR) vaccine, diphtheria/tetanus/pertussis (DTP) vaccine, quadrivalent influenza vaccine, nonavalent human papillomavirus (HPV) vaccine, and trivalent inactivated poliovirus vaccine, has protected human health worldwide. Previous reports have demonstrated that the monovalent EV-A71 vaccine poorly neutralizes the CVA16 virus [27]. To offer broad protection to HFMD patients, it is considered essential to include the CVA16 antigen to form multivalent vaccine formulations [28–31].

In this study, we constructed a DNA-launched CVA16 infectious clone to minimize the interference of viral quasispecies and used a serum-free suspension of the HEK293A culture system to improve production yields. We investigated the biochemical and immunological properties of DNA-launched CVA16 infectious clone and observed its growth kinetics in different cell lines. In addition, the bivalent vaccine approach was also evaluated with EV-A71 antigens in an animal model. These findings are expected to contribute to HFMD vaccine development.

Materials and methods

Cells, media, and viruses

Rhabdomyosarcoma (RD) cells were purchased from the Bioresource Collection and Research Center (BCRC), Hsinchu, Taiwan. Human embryonic kidney 293 adherent (HEK293A) cells were purchased from Invitrogen (Cat. R70507). RD and HEK293A cells were cultured in Dulbecco's modified Eagle's medium (DMEM, Gibco) supplemented with 10 % fetal bovine serum (FBS). Vero (CCL-81) cells, obtained from the American Type Culture Collection (ATCC, USA), were grown in VP-SFM medium (Gibco). Serum-free adapted HEK293A cells were cultured in BalanCD HEK293 medium (FUJIFILM Irvine Scientific) in suspension, as described previously [14]. The CVA16 N5079 strain (CVA16wt, GenBank: AF177911.1) was obtained from National Cheng Kung University Hospital (NCKUH), Taiwan. The EV-A71 E59 strain was obtained from the Centers for Disease Control (CDC), Taiwan.

Viral RNA extraction, RT-PCR, and genome sequencing

Viral RNAs were extracted from 400 μL of viral supernatant using NucleoZOL (Macherey-Nagel) according to the manufacturer's instructions. Extracted RNAs were resuspended in 50 μL DEPC-treated water. Reverse transcription was performed using 2 μL of viral RNA with the RevertAid H Minus First Strand cDNA Synthesis Kit (ThermoFisher Scientific). Viral cDNA was amplified using the KOD −Plus- Neo kit (TOYOBO) with primers F: CCATATAGCTATTGGATTGGCCATCC and R: TCATCCAGCCATAGAAGATCTCTGA. PCR products were purified using the FavorPrep GEL/PCR Extraction or Purification DNA Fragments Mini Kit (Favorgen) and sequenced at the Core Instrument Center, National Health Research Institutes (NHRI), Taiwan.

Cloning and assembly of full-length CVA16 viral genome

The recombinant DNA application (NHRI-IBC-101018) was reviewed and approved by the Institutional Biosafety Committee of NHRI. The full-length CVA16 genome was divided into 4 contiguous fragments (F1 to F4) based on unique restriction enzyme sites (Table 1). Two silent mutations (T1162C and C3019G) were engineered in the capsid protein region by site-directed mutagenesis PCR to differentiate the infectious clone-derived virus from the clinical isolate. A poly(A)$_{30}$ tail was added after the 3′ untranslated region of the viral genome. Each fragment was amplified by PCR and cloned into the pUC19 shuttle vector (pUC19-F1, pUC19-F2, pUC19-F3, and pUC-F4). All subclones were validated by Sanger sequencing.

The assembly of F1 to F4 fragments into the full-length viral genome was performed in two steps. First, F2 and F4 fragments were digested from their respective plasmids and cloned into pUC19-F1 and pUC19-F3 plasmids, resulting in pUC19-F1/F2 and pUC19-F3/F4. Second, the F1/F2 and F3/F4 fragments were prepared following the same procedure and simultaneously cloned into a modified pCMV-HA vector (Clontech). During the assembly process, all digested plasmids underwent agarose gel separation, excision, and DNA purification. Ligation was performed using T4 ligase (ThermoFisher Scientific) at 4 °C overnight. The structure of the CVA16 infectious clone (CVA16ic) plasmid (pFL-CVA16-N5079) is shown in Fig. 1A.

DNA transfection, virus recovery, determination of viral titer, and plaque assay

The pFL-CVA16-N5079 plasmid was transfected into RD cells using homemade polyethylenimine reagent (PEI) to recover the virus. Two μg of plasmid were mixed with 8 μL of PEI solution and added to a well containing 1×10^6 RD cells in 6-well plates. At 96 h post-transfection, half of the culture medium was transferred to fresh RD cells, followed by a medium exchange after 1 h of incubation. At 3 days post-infection (DPI), the first passage (P1) virus was harvested as the CVA16ic master bank. The second passage (P2) virus was produced by inoculating 10 μL of P1 virus into a T-75 flask containing 90 % confluent Vero cells in fresh VP-SFM medium. Cells were observed for virus-induced cytopathic effect (CPE), and the culture medium containing P2 virus was harvested at 6 DPI as the working bank.

The P2 virus titer was determined by the median tissue culture infectious dose ($TCID_{50}$) assay. Serially diluted virus samples (10^{-1} to 10^{-8}) were added to RD cells growing in 96-well plates and incubated for six days at 37 °C. $TCID_{50}$ values were calculated using the Reed-Muench method after counting the CPE. For plaque assays, 100 μL of 10-fold serially diluted culture supernatants were added to monolayers of RD cells in 6-well plates. After 1 h of incubation at 37 °C, 4 mL of medium containing 10 % FBS and 1.2 % methylcellulose was added to each well.

Table 1
Primers used for the construction of the CVA16 infectious clone.

Fragment	Primer	Sequence (5′to 3′)
F1	NotI_1F	AATCGCGGCCGCTTAAAACAGCCTGTGGGTTGTTC
	1R_SalI	GCTTGTCGACTGCCGTTGCATCTGTGTCTGGGCA
F2	SalI_2F	GGCAGTCGACAAGCCTACACGACCTGACGTGTCA
	2R_EcoRV	GATTGATATCTAGCTGGGTAATACTCACTAGCT
F3	EcoRV_3F	GCTAGATATCAATCCCATCTCATGCTTGCTGTG
	3R_KpnI	TAGGGGTACCCGGCGCTAGTGTGCAGGTCTATG
F4	KpnI_4F	GCCGGGTACCCCTATAGTGCCTTGGGTGTTAAGAA
	4R_NotI	CGATGCGGCCGCTTTTTTTTTTTTTTTTTTTTTTTTTTTTTTTTTTGCTATTCTGGTTATAACAAATTTACCCCC

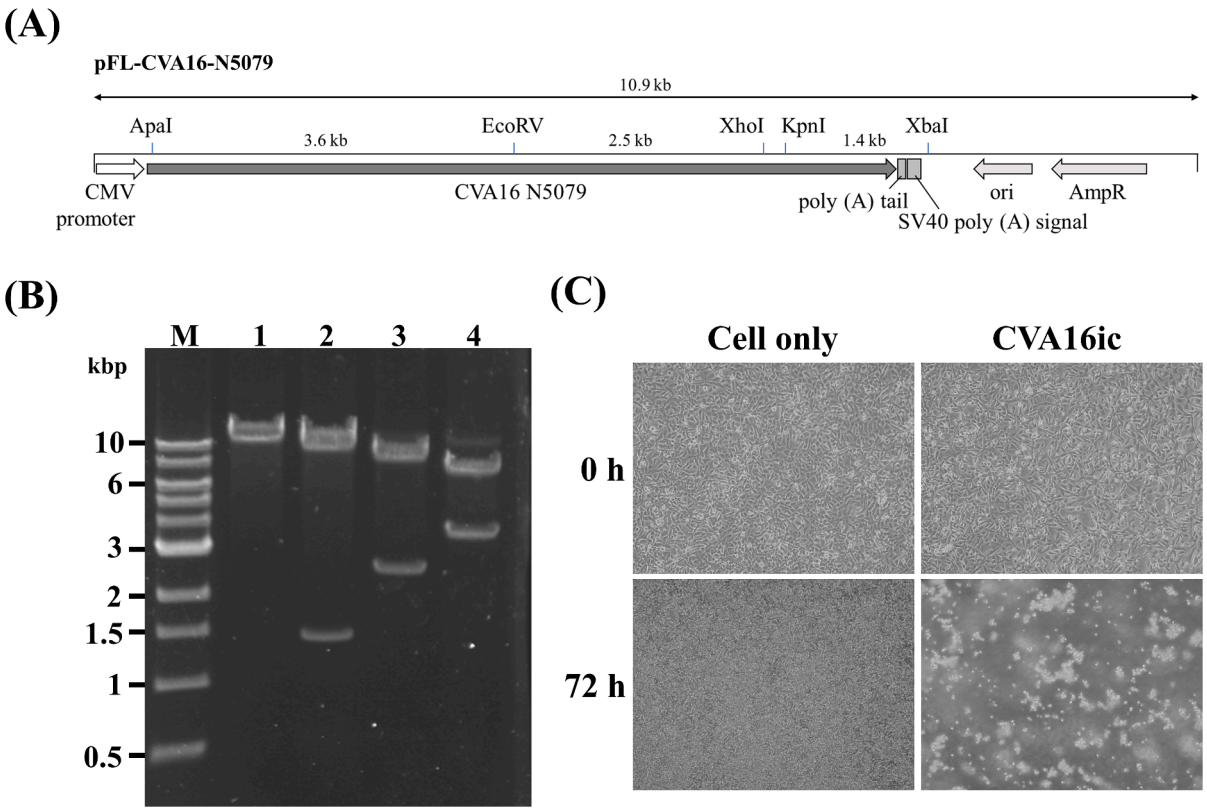

Fig. 1. Construction of CVA16 infectious clone. (A) Structure of the CVA16ic plasmid. The pFL-CVA16-N5079 plasmid contains full-length CVA16 N5079 cDNA inserted into a modified pCMV-HA vector. (B) Agarose gel analysis of the CVA16ic plasmid digested by restriction enzymes XbaI (lane 2), XbaI/KpnI (lane 3), XhoI/EcoRV (lane 4), and ApaI/EcoRV (lane 5). A DNA ladder (M) was included in lane 1. (C) Cytopathic effects induced by CVA16ic P2 virus infection in RD cells at 3 DPI. RD cells were seeded at 5×10^5 cells per well in 6-well plates 24 h before virus infection. The medium was replaced with 1 mL of CVA16ic P1 virus-containing medium (directly from transfected cells) for 1 h, followed by replacement with 2 mL of fresh medium.

After 3 days of incubation, plaques were stained using naphthol blue-black dye.

Virus growth in roller bottle and suspension system

Vero cells were seeded at 1×10^7 cells per roller bottle in VP-SFM medium. At 80–90 % confluence, the medium was refreshed (working volume: 333 mL), and cells were infected with CVA16 at multiplicities of infection (MOI) of 10^{-3}, 10^{-4}, and 10^{-5}. HEK293A suspension cells were seeded at a density of 1×10^6/mL in a 250 mL spinner flask with 50 mL of fresh BalanCD HEK293 medium and infected with CVA16 at the same MOIs. Replication kinetics of CVA16 in both systems were measured using the $TCID_{50}$ assay.

CVA16 viral particle preparation

For purification of CVA16ic viral particles, 1 L of CVA16ic harvest was cultured using the HEK293A suspension system. The harvest underwent three freeze/thaw cycles and was concentrated to 50 mL using a tangential flow filtration (TFF) cassette (Sartorius). CVA16ic viral particles were isolated by 10 to 60 % continuous sucrose gradient centrifugation (32,000 rpm, 3 h). For SDS-PAGE, CVA16ic proteins were separated on a 4–12 % gradient gel (Invitrogen) and silver-stained using the SilverXpress kit (Invitrogen). For western blot analysis, proteins were transferred onto a PVDF membrane (Invitrogen). Anti-CVA6 VP1 antibody GTX132346 (GeneTex) and EV-A71 antibody mAb979 (Millipore) were used to detect CVA16ic VP1 and VP2 proteins, respectively, as described previously [14]. LumiFlash Ultima Chemiluminescent Substrate, HRP System (Visual Protein) was used for chemiluminescence development. Viral particles were concentrated and buffer-exchanged into phosphate-buffered saline (PBS) using 100 k MWCO Amicon centrifugal filter tubes (Millipore). CVA16ic viral particles were inactivated with 1/4000 (v/v) formaldehyde at 37 °C for 3 days. Inactivated particles were stained with 2 % uranyl acetate for JEM-1400 TEM inspection. The purification of CVA16ic empty (E-) and full (F-) particles through sucrose gradient ultracentrifugation, SDS-PAGE, western blot,

and transmission electron microscopy (TEM) were performed as described previously [14].

Immunogenicity studies and virus neutralizing test

Animal experiments were reviewed and approved by the Institutional Animal Care and Use Committee of NHRI (Approval no. NHRI-IACUC-111034-A-S02). Six female BALB/c mice (6 weeks old) per group were immunized intramuscularly with 0.1 mL of antigen (0.5 μg viral particle adjuvanted with 60 μg aluminum phosphate). Formalin-inactivated EV-A71 bulk (sample-05) was obtained from NHRI PIC/S GMP facility for the bivalent group [32]. EV-A71 bulk (0.5 μg) was mixed with CVA16ic F-particle (0.5 μg) and prepared with 60 μg aluminum phosphate in 0.1 mL. The immunization regimen consisted of two doses administered at two-week intervals. Blood samples were collected one week after the secondary dose and inactivated at 56 °C for 30 min. Neutralizing antibody titers (Nt titer) were determined as described previously [14].

Endpoint ELISA assay

Antigen-specific IgG titers of mouse antisera were determined by ELISA, with mAb979 (2-fold serial dilution) serving as a positive control antibody. ELISA plates were coated with CVA16ic particles (100 ng/well in 50 μL coating buffer: 1 M NaHCO3, pH 9.5). Serially diluted mouse sera samples (10^2 to 10^6 dilutions) were added to the plates and incubated for 2 h at room temperature. Wells were washed four times with 200 μL of wash buffer (PBS+0.05 % Tween20) and incubated with 100 μL of anti-mouse IgG-HRP secondary antibody (1:5000) for 1 h at room temperature. After six washes, 50 μL of TMB peroxidase substrate (SureBlueTM, KPL) was added for 0.5 h, and the reaction was stopped with 50 μL of 2 N sulfuric acid. Absorbance at 450 nm was measured using an ELISA reader (Spectra Max M2 model, USA). The endpoint titer was determined as the highest dilution fold at which the absorbance was at least four times higher than the background signal.

Statistical analysis

Numerical data are presented as mean ± standard deviation (SD). Group comparisons of endpoint ELISA and viral neutralizing antibody titers in Figs. 5 and 6 were performed using one-way ANOVA. Differences in the replication kinetics of CVA16 virus in Vero and suspension HEK293A cells were analyzed with multiple t-tests. Significance levels: $p > 0.05$, ns (not significant); *$p < 0.05$; **$p < 0.01$; ***$p < 0.001$.

Results

Construction of the DNA-launched CVA16 infectious clone

To confirm the presence of the full genome of the CVA16 N5079 strain cloned and inserted into the vector, we conducted diagnostic restriction digestion analysis, as shown in Fig. 1A and B. The full-length of the pFL-CVA16-N5079 plasmid is nearly 10.9 Kbp, and the observed sizes of the digested DNA fragments matched our predictions. Subsequently, we transfected this CVA16ic plasmid into RD cells to recover the recombinant CVA16 virus. The successful recovery of CVA16ic was confirmed by transferring the culture supernatant to fresh RD cells at 96 h post-transfection, resulting in the observation of obvious CPEs at 72 h (Fig. 1C). These results show the generation of an infectious plasmid containing the full-length CVA16 N5079 genome and the successful recovery of the CVA16ic virus.

Identification of the CVA16ic virus in different cell lines

To identify whether CVA16ic differs from the original CVA16wt, viral infectivity was assessed in several cell lines, including RD, Vero, and HEK293A cells. Both CVA16ic and CVA16wt induced CPE in RD, Vero, and HEK293A cells (Fig. 2A). Western blot analysis of these culture supernatants revealed the presence of both CVA16ic and CVA16wt proteins using the VP1 and the VP2 antibodies, indicating efficient propagation in these cell lines. EV-A71, as a control virus, was detected using the VP2 antibody in all tested cell lines, while no signal was detected when using the VP1 antibody, consistent with our previous report (Fig. 2B) [14]. In viral plaque assays, the developed plaques of CVA16ic were similar to those of CVA16wt (Fig. 2C). Sequencing of the capsid proteins confirmed the stable preservation of two engineered mutations in CVA16ic, with no other sequence changes observed, suggesting that our CVA16ic preparation was not contaminated by CVA16wt (Fig. 2D and E). Taken together, these results demonstrate that CVA16ic exhibits characteristics identical to those of CVA16wt.

Evaluation of CVA16 production in different cell culture systems

Considering that standard EV-A71 vaccine production typically employs Vero cells and serum-free VP-SFM media, we also evaluated the growth kinetics of CVA16ic and CVA16wt under the same conditions. Vero cells were seeded into roller bottles and infected with CVA16ic (Fig. 3A to C) or CVA16wt (Fig. 3D to F) at MOIs of 10^{-3}, 10^{-4}, or 10^{-5}. Both viruses exhibited similar replication kinetics, with virus titers peaking at 1–2 × 10^5 $TCID_{50}$/mL after 3 to 6 DPI (Fig. 3, black bars). To improve CVA16 virus yield, we also evaluated the replication of CVA16ic and CVA16wt in a serum-free HEK293A suspension system. In this system, both CVA16ic and CVA16wt reached peak titers of 1–5 × 10^7 $TCID_{50}$/mL after 4 DPI at all tested MOIs (10^{-3}, 10^{-4}, and 10^{-5}) (Fig. 3, grey bars). These results demonstrate that the serum-free HEK293A suspension system could produce up to 100-fold higher titers compared to the serum-free Vero cell system, suggesting it as a more efficient propagation system for CVA16 production.

Purification of CVA16ic particles from serum-free HEK293A suspension culture system

Two naturally occurring major enterovirus particles, immature E-particles and mature F-particles, demonstrate structural and immunological differences. To purify the E- and F-particles of CVA16ic from the serum-free HEK293A suspension culture system, concentrated CVA16ic was subjected to 10 to 60 % continuous sucrose gradient ultracentrifugation. The sucrose gradient fractions were collected and analyzed using the VP2 antibody. Virus particles were identified in two regions (Fig. 4A). Based on the predicted protein sizes of VP0 (35.9 kDa) and VP2 (28.2 kDa), the E-particle of CVA16ic was located in fraction 6 to 7, and the F-particle of CVA16ic was located in fraction 12 to 13. The E- and F-particle fractions were concentrated and buffer-exchanged to become the final E- and F-particles, respectively. Silver staining analysis revealed the successful separation of the two CVA16ic particles; no VP2 was detected in the E-particle samples and no VP0 was detected in the F-particle samples (Fig. 4B). TEM revealed the morphologies of the purified CVA16ic E- and F-particles, which exhibited diameters ranging from 30 to 35 nm (Fig. 4C). These data indicate that the CVA16ic viral particles produced in HEK293A cells were similar to those produced in Vero cells in our previous study [5].

Immunogenicity studies of CVA16ic particles and bivalent antigens with EV-A71

To evaluate the immunogenicity of CVA16ic produced from the serum-free HEK293A suspension system, mice were immunized with formalin-inactivated E- and F-particles of CVA16ic, and neutralizing antibody assays were performed (Fig. 5). Mice immunized with the CVA16ic E-particle did not generate detectable neutralizing antibodies. In addition, immunization with the CVA16ic F-particle also failed to induce detectable neutralizing antibodies. Given the potential of

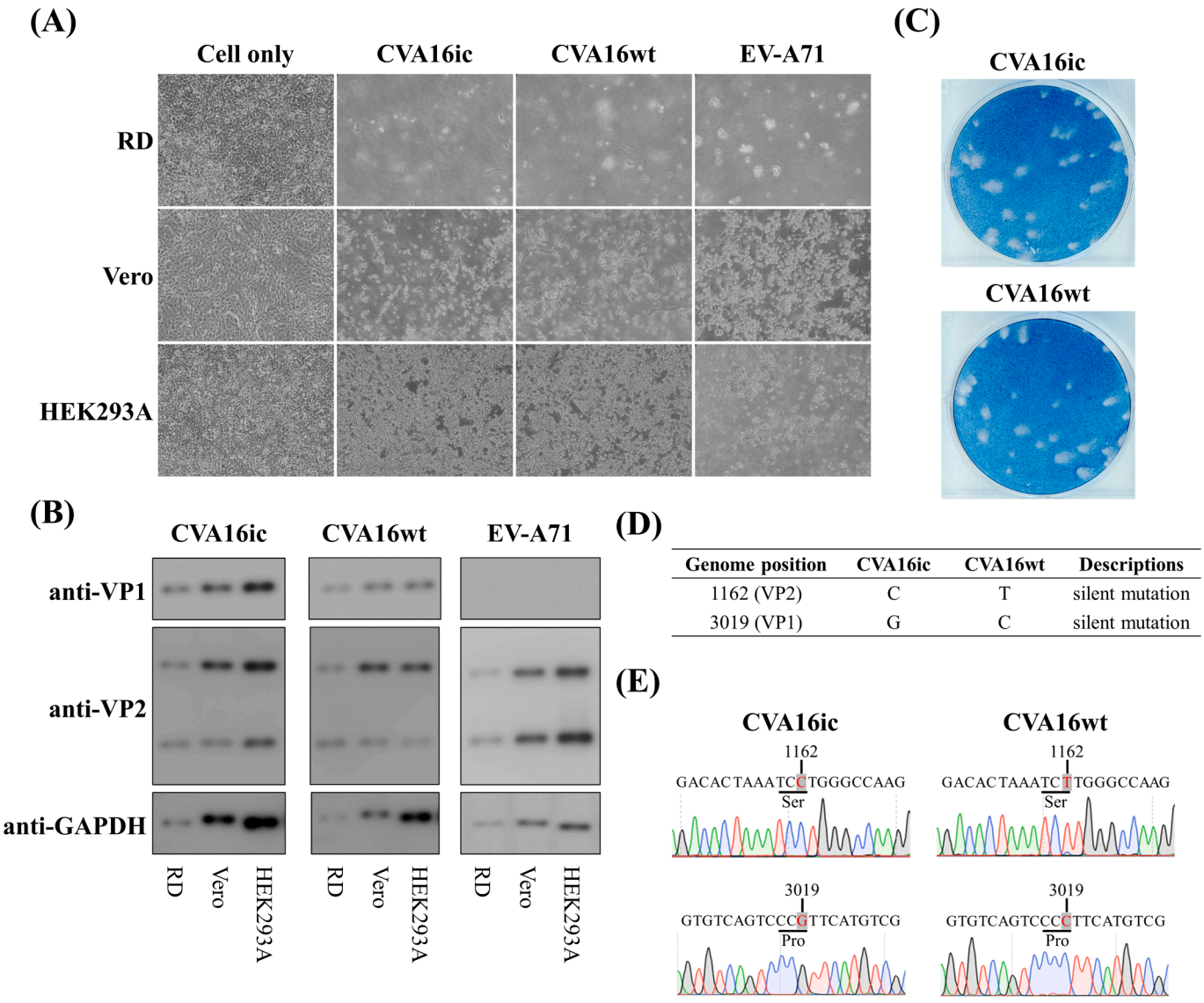

Genome position	CVA16ic	CVA16wt	Descriptions
1162 (VP2)	C	T	silent mutation
3019 (VP1)	G	C	silent mutation

Fig. 2. Characterization of the CVA16ic virus. (A) Susceptibility of RD, Vero, and HEK293 cells to CVA16 and EV-A71 viruses. All cell lines were seeded at 2.5×10^5 cells per well in 6-well plates 24 h prior to viral infection. The cells were infected with CVA16wt, CVA16ic, and EV-A71 viruses at MOI=10^{-3}. Infected cells were observed at 4 DPI. (B) Western blot analysis of samples collected from infected cells at 4 DPI. Ten μL of culture supernatant were loaded and detected with the VP1 (GTX132346) and the VP2 (mAb979) antibodies. The GAPDH antibody served as a loading proof control, but not for normalization due to different expression levels in these cell lines. (C) Plaque morphology of CVA16ic and CVA16wt. Vero cells were used to adsorb the two CVA16 viruses, and the overlay medium contained 1.2 % methylcellulose for plaque development. (D) Nucleotide differences in the capsid protein between CVA16ic and CVA16wt. Two silent mutations were engineered as molecular markers. (E) Sequencing results showing the retention of molecular markers in the virus working bank.

bivalent EV-A71 and CVA16 vaccination to provide broader protection against HFMD, mice were also immunized simultaneously with CVA16ic F-particle and EV-A71 bulk. The results revealed that the antisera of bivalent antigens exhibited a robust neutralizing antibody response against both CVA16 and EV-A71 viruses. In addition, bivalent antigens elicited a higher neutralizing titer against EV-A71 (Nt = 2277.3) than against CVA16 (Nt = 172.9). Notably, monovalent EV-A71 antisera exhibited poor neutralization (Nt < 16) of the CVA16 virus. These findings indicate that CVA16-neutralizing antibodies are generated in response to the CVA16ic F-particle and that EV-A71 plays a crucial role in conferring its immunogenicity.

Anti-CVA16-specific antibody responses in mouse antisera

An endpoint ELISA was also conducted to confirm the specific antibody responses generated from the vaccinated mice (Fig. 6A and B). Interestingly, neither aluminum phosphate-adjuvanted CVA16ic E-particles nor F-particles elicited detectable antibodies to CVA16ic and EV-A71 particles. However, antisera from the bivalent group displayed both CVA16-specific and EV-A71-specific antibodies. Notably, antisera from mice immunized with EV-A71 also reacted with CVA16 particles, although these antibodies were nonneutralizing (Fig. 5). These results indicate that monovalent CVA16ic F-particles are not sufficient to induce specific immune responses against CVA16 and could be improved by combination with the EV-A71 antigen.

Discussion

RNA viruses are known to undergo broad virus diversification and accumulate mutations during replication [33]. While plaque-to-plaque purification is commonly used to isolate a pure virus strain from a population pool, there are still minor populations consisting of purified viruses with similar genomes. In contrast, infectious clones provide a solution by generating viruses through the transfection of virus genomes

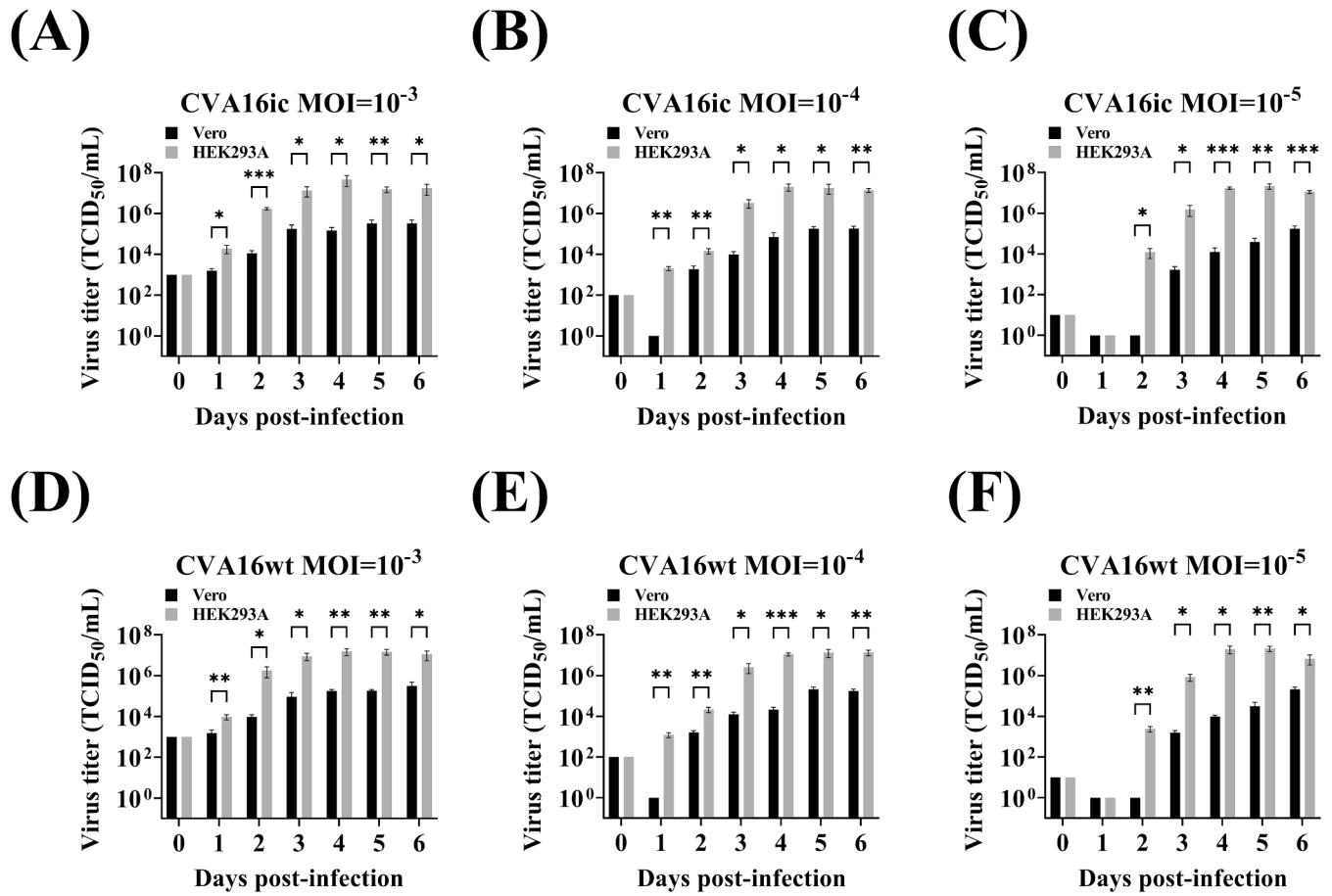

Fig. 3. Replication kinetics of two CVA16 viruses in Vero and HEK293A culture systems. Replication kinetics of CVA16ic and CVA16wt viruses were measured in Vero cells and HEK293A suspension cells. Vero cells were seeded in roller bottles with VP-SFM medium, and HEK293A cells were seeded at a density of 1×10^6 cells/mL in a 250 mL spinner with BalanCD293 medium. CVA16ic (A to C) or CVA16wt (D to F) infected both cell types at MOIs of (A and D) 10^{-3}, (B and E) 10^{-4}, and (C and F) 10^{-5}. The $TCID_{50}$ values were calculated using the Reed-Muench method, and results from triplicate experiments are presented with error bars indicating standard deviations.

into host cells, resulting in viruses with limited passage numbers and clearly defined sequences. The typical construction of an infectious clone for *enteroviruses* involves cloning the full-length viral cDNA genome under a bacteriophage promoter, either T7 or SP6 [4]. Subsequently, viral RNA is generated using T7 or SP6 RNA polymerase *in vitro* and transfected into host cells to recover live virus. However, this procedure requires additional steps, including *in vitro* transcription, capping RNA with a 5′ cap, and RNA purification, which are time-consuming. In this study, we developed a DNA-launched CVA16 infectious clone using the CMV promoter, facilitating the direct transcription of the CVA16 viral genome by RNA polymerase II in mammalian cells (Fig. 1C). This approach eliminates the need for *in vitro* RNA transcription, thereby reducing quality risk and ensuring quality, as in our previous study [17]. Several characteristic analyses demonstrated no significant difference between CVA16ic and CVA16wt (Fig. 2). All these characteristics enhance quality control and quality risk management in cGMP compliance during vaccine manufacturing.

Vero cells are among the most common cell lines utilized in the production of viral vaccines, with more than 40 years of mature experience in the vaccine industry [34]. Licensed vaccines for viruses such as poliomyelitis, Japanese encephalitis virus (JEV), EV-A71, and influenza virus are examples of Vero cell-based vaccines [35]. In this study, we demonstrated the inefficient replication of the CVA16 virus in Vero cells, with viral titers plateauing at approximately 10^5 $TCID_{50}$/mL (Fig. 3). An inadequate production yield of CVA16 results in increased manufacturing costs, which affects CVA16 vaccine development. Recently, a serum-free HEK293A suspension system was established to facilitate the growth of several enteroviruses, which could improve enterovirus manufacturing [14]. Western blot analysis also implicated that, compared with Vero cells, HEK293A cells produced the CVA16 virus more efficiently (Fig. 2B). Therefore, we confirmed the production of the CVA16 virus under low-MOI conditions in this system, resulting in enhanced viral titers of more than 10^7 $TCID_{50}$/mL (Fig. 3). We further demonstrated that the biochemical analysis of HEK293A-produced CVA16ic was similar to that of Vero-produced CVA16wt [5]. HEK293 cell lines have also been used to produce several FDA/EMA-approved biologics, including SARS-CoV-2 vaccines [36,37]. According to our results, HEK293A suspension cells could be a promising culture system for CVA16 production. In addition, unlike the adherent Vero cell system, the serum-free HEK293A system operates in suspension which offers advantages in scaling up during the manufacturing process.

During the life cycle of human enteroviruses, two major particle forms exist, namely, E-particles and F-particles, which exhibit significant differences in infectivity and immunogenicity [5,38]. We separated E- and F-particles using ultracentrifugation and confirmed their immunogenicity. Neither the E-particle nor the F-particle of CVA16ic from the HEK293A cell culture elicited specific neutralizing antibodies ($Nt < 16$) (Fig. 5). We also purified these CVA16ic particles produced in Vero cells and obtained the same results in the immunogenicity study (data not shown). Similar inefficiencies in generating neutralizing antibodies have also been reported for other currently circulating CVA16 strains, both in live and inactivated forms [13]. Although some studies have shown that

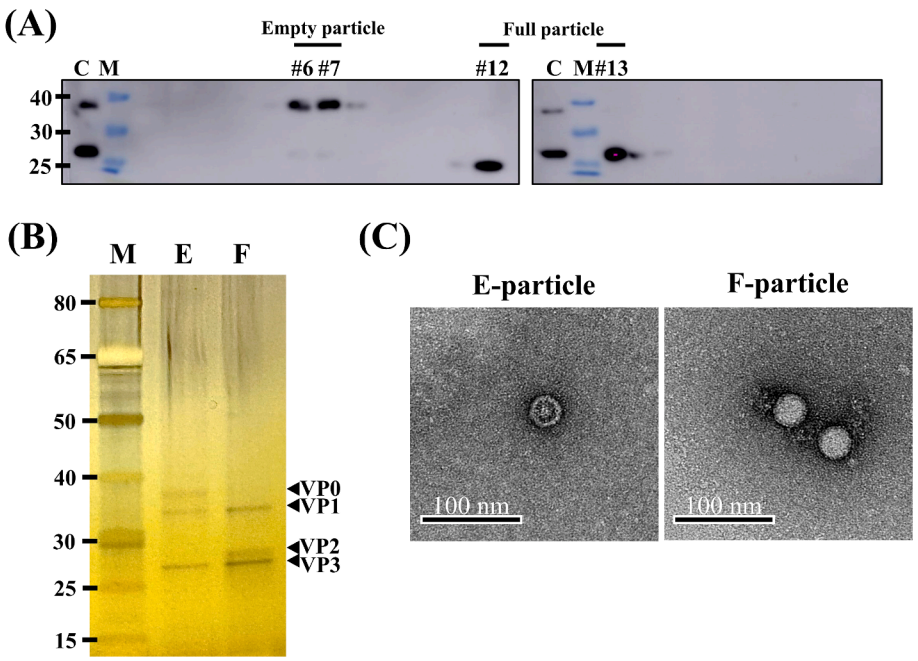

Fig. 4. Purification and characterization of CVA16ic E- and F-particles. (A) Purification of CVA16ic by 10–60 % sucrose gradient zonal ultracentrifugation. M: protein ladder; C: sample loaded with CVA16ic from culture medium. The CVA16ic antigen was detected with the VP2 antibody. The numbers below the panels indicate the fractions collected during elution, and the numbers next to the protein ladder indicate protein sizes. CVA16ic antigen after ultracentrifugation was analyzed by western blotting. (B) Protein profiles of the purified CVA16ic E- and F-particles using SDS-PAGE 4–12 % gel. M: protein ladder; E: E-particle from fraction 6; and F: F-particle from fraction 13. (C) CVA16ic E-particles (left) and F-particles (right) analyzed by TEM. The scale bar represents 100 nm.

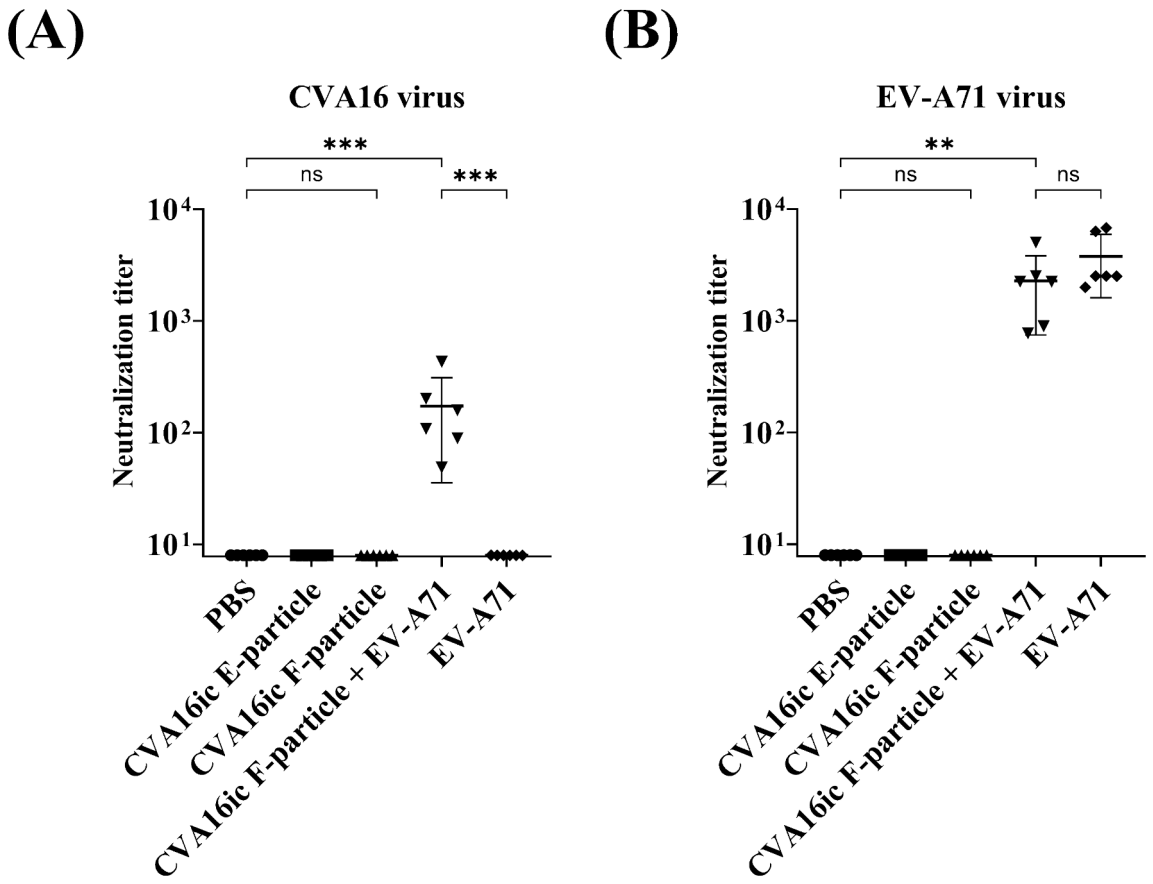

Fig. 5. Neutralizing antibody titers in mice. Sera from mice immunized with mock (PBS), CVA16 E-particle, CVA16 F-particle, and bivalent CVA16 F-particle and EV-A71 antigen were evaluated for neutralizing antibody titers against (A) CVA16 virus and (B) EV-A71 virus.

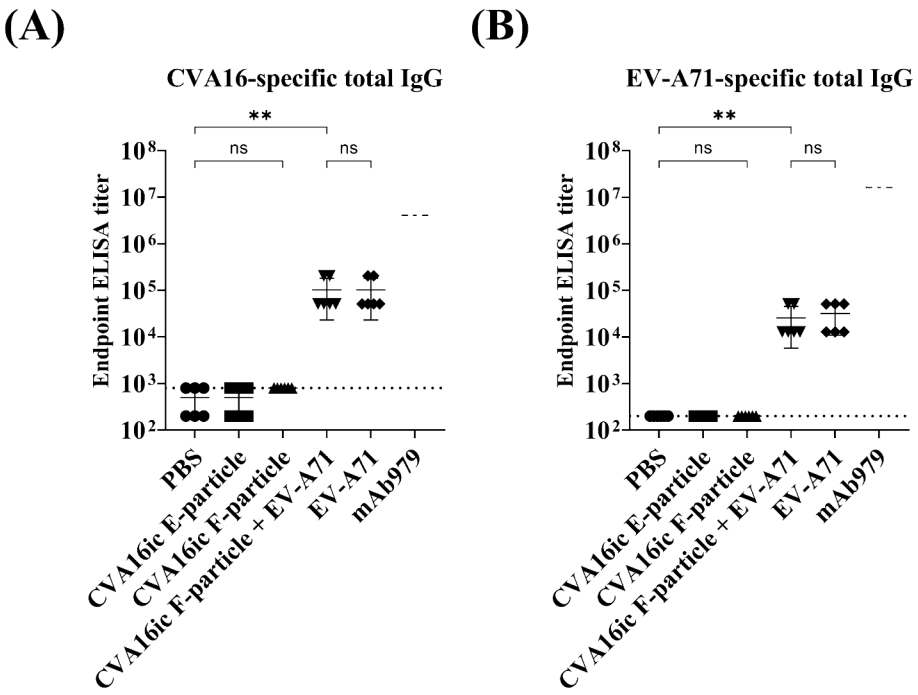

Fig. 6. Specific antibody titers in mice antisera. Sera from mice immunized with mock (PBS), CVA16 E-particle, CVA16 F-particle, and bivalent CVA16 F-particle and EV-A71 antigen were evaluated for specific antibody titers against (A) CVA16 virus and (B) EV-A71 virus.

inactivated CVA16 particles can induce protective antibodies, the titers remain mild [39,40]. These data collectively suggest the low immunogenic nature of the CVA16 virus and the difficulties encountered in the development of monovalent CVA16 vaccine candidates.

The development of vaccines against HFMD has predominantly focused on EV-A71, with five inactivated EV-A71 monovalent vaccines licensed by local regulatory authorities [3,32]. However, these EV-A71 vaccines have demonstrated ineffectiveness against CVA16, highlighting their conformational specificity. In this study, we also performed bivalent immunization targeting both CVA16 and EV-A71. Surprisingly, when CVA16ic F-particle was combined with the EV-A71 antigen, a significant CVA16-specific neutralizing antibody titer was detected, whereas the EV-A71 antigen alone failed to induce neutralizing antibodies against CVA16 (Fig. 5). Initially, we attributed the loss of immunogenicity of our inactivated CVA16ic F-particles to potential antigenicity alterations during formalin inactivation. However, the bivalent group raised the possibility that CVA16ic F-particle is antigenic, but aluminum phosphate may not be an optimal adjuvant for CVA16. Indeed, endpoint-ELISA analysis confirmed that sera from mice immunized with CVA16ic F-particle did not exhibit specific recognition of CVA16 antigens (Fig. 6A). EV-A71 particles induced high neutralizing antibody titers against EV-A71, and these antibodies also cross-reacted with CVA16 particles but displayed poor neutralizing ability against CVA16 (Figs. 5 and 6) [27]. Therefore, CVA16 neutralizing antibodies could result from CV-A16ic F-particle during bivalent CVA16 and EV-A71 immunization. These data indicate that the EV-A71 antigen may play dual roles in bivalent antigen immunization, providing protection against EV-A71 and enhancing the immunogenicity of CVA16ic F-particles. Furthermore, our low-immunogenicity CVA16ic F-particle may serve as a valuable material for formulation research in the development of enterovirus vaccines.

In conclusion, we generated a recombinant CVA16 virus from a CMV promoter-driven infectious clone that is antigenic for bivalent HFMD vaccine development. We also demonstrated that serum-free HEK293A suspension cells are a more efficient cell culture system for CVA16 production. In addition, our study showed that inactivated EV-A71 antigens could enhance the immunogenicity of inactivated CVA16 F-particle, suggesting that a bivalent CVA16 and EV-A71 vaccine may be an effective strategy for CVA16 vaccine development. We expect our findings to provide novel strategies and accelerate the development of HFMD vaccines.

Declaration of generative AI and AI-assisted technologies in the writing process

During the preparation of this work the author(s) used Claude, an artificial intelligence language model developed by Anthropic, solely to assist with English grammar and language editing. Claude was not involved in any aspect of the research design, data analysis, interpretation of results, or drafting of scientific content. After using this tool/service, the author(s) reviewed and edited the content as needed and take(s) full responsibility for the content of the published article.

CRediT authorship contribution statement

Yi-An Chen: Writing – original draft, Methodology, Investigation, Conceptualization. **Yu-Sheng Shen:** Investigation. **Chih-Yeu Fang:** Formal analysis. **Ting-Ting Chan:** Investigation. **Shang-Rung Wu:** Investigation. **Jen-Ren Wang:** Resources. **Suh-Chin Wu:** Resources. **Chia-Chyi Liu:** Writing – review & editing, Writing – original draft, Project administration, Methodology, Funding acquisition, Formal analysis, Data curation, Conceptualization.

Declaration of competing interest

The authors declare that they have no known competing financial interests or personal relationships that could have appeared to influence the work reported in this paper.

Data availability

Data will be made available on request.

Acknowledgements

This work was supported by the Ministry of Health and Welfare, the Taiwan CDC and the National Health Research Institutes (10A1-IVPP16-014, 11A1-IVPP14–014, 12A1-IVPP18-014, 13A1-IVPP20-014), Taiwan. We thank Core Instrument Center of the National Health Research Institutes to provide DNA sequence service. We also thank the technical services provided by "the i-MANI center of the National Core Facility for Biopharmaceuticals, Ministry of Science and Technology, Taiwan" as well as the technical service from the Instrument Development Center of the National Cheng Kung University. The first author: Yi-An Chen carried out his/her thesis research under the auspices of the Graduate Program of Biotechnology in Medicine, National Tsing Hua University and National Health Research Institutes.

References

[1] Mao Q, Wang Y, Yao X, Bian L, Wu X, Xu M, et al. Coxsackievirus A16: Epidemiology, diagnosis and vaccine. Hum Vaccin Immunother 2014;10:360–7.
[2] Klein M, Chong P. Is a multivalent hand, foot, and mouth disease vaccine feasible? Hum Vaccin Immunother 2015;11:2688–704.
[3] Fang CY, Liu CC. Recent development of enterovirus A vaccine candidates for the prevention of hand, foot, and mouth disease. Expert Rev Vaccines 2018;17:819–31.
[4] Fang CY, Liu CC. Novel strategies for the development of hand, foot, and mouth disease vaccines and antiviral therapies. Expert Opin Drug Discov 2022;17:27–39.
[5] Chong P, Guo MS, Lin FH, Hsiao KN, Weng SY, Chou AH, et al. Immunological and biochemical characterization of coxsackie virus A16 viral particles. PLoS One 2012; 7:e49973.
[6] Liu Q, Yan K, Feng Y, Huang X, Ku Z, Cai Y, et al. A virus-like particle vaccine for coxsackievirus A16 potently elicits neutralizing antibodies that protect mice against lethal challenge. Vaccine 2012;30:6642–8.
[7] Cai Y, Liu Q, Huang X, Li D, Ku Z, Zhang Y, et al. Active immunization with a Coxsackievirus A16 experimental inactivated vaccine induces neutralizing antibodies and protects mice against lethal infection. Vaccine 2013;31:2215–21.
[8] Yang E, Cheng C, Zhang Y, Wang J, Che Y, Pu J, et al. Comparative study of the immunogenicity in mice and monkeys of an inactivated CA16 vaccine made from a human diploid cell line. Hum Vaccin Immunother 2014;10:1266–73.
[9] Lin CW, Liu CC, Lu TC, Liu SJ, Chow YH, Chong P, et al. Immunogenicity studies of bivalent inactivated virions of EV71/CVA16 formulated with submicron emulsion systems. Biomed Res Int 2014;2014:670506.
[10] Sun S, Jiang L, Liang Z, Mao Q, Su W, Zhang H, et al. Evaluation of monovalent and bivalent vaccines against lethal Enterovirus 71 and Coxsackievirus A16 infection in newborn mice. Hum Vaccin Immunother 2014;10:2885–95.
[11] Yang T, Xie T, Li H, Song X, Yue L, Wang X, et al. Immune responses of a CV-A16 live attenuated candidate strain and its protective effects in rhesus monkeys. Emerg Microbes Infect 2020;9:2136–46.
[12] Wang J, Zhang Y, Zhang X, Hu Y, Dong C, Liu L, et al. Pathologic and immunologic characteristics of coxsackievirus A16 infection in rhesus macaques. Virology 2017; 500:198–208.
[13] Yao X, Mao Q, Li Y, Hao C, Bian L, Chen P, et al. Poorly neutralizing polyclonal antibody in vitro against coxsackievirus A16 circulating strains can prevent a lethal challenge in vivo. Hum Vaccin Immunother 2018;14:1275–82.
[14] Lien SC, Shen YS, Lin HY, Wu SR, Fang CY, Chen CH, et al. Propagation and immunological characterization of coxsackievirus A10 in a serum-free HEK293A cell culture system. Virus Res 2023;329:199101.
[15] Bray M, Lai CJ. Construction of intertypic chimeric dengue viruses by substitution of structural protein genes. Proc Natl Acad Sci USA 1991;88(22):10342–6.
[16] Neumann G, Fujii K, Kino Y, Kawaoka Y. An improved reverse genetics system for influenza A virus generation and its implications for vaccine production. Proc Natl Acad Sci USA 2005;102:16825–9.
[17] Yang YT, Chow YH, Hsiao KN, Hu KC, Chiang JR, Wu SC, et al. Development of a full-length cDNA-derived enterovirus A71 vaccine candidate using reverse genetics technology. Antiviral Res 2016;132:225–32.
[18] Xie X, Muruato A, Lokugamage KG, Narayanan K, Zhang X, Zou J, et al. An Infectious cDNA Clone of SARS-CoV-2. Cell Host Microbe 2020;27:841.
[19] Nogales A, Martínez-Sobrido L. Reverse Genetics Approaches for the Development of Influenza Vaccines. Int J Mol Sci 2016;18:20.
[20] Liu F, Liu Q, Cai Y, Leng Q, Huang Z. Construction and characterization of an infectious clone of coxsackievirus A16. Virol J 2011;8:534.
[21] Deng C, Li X, Liu S, Xu L, Ye H, Qin CF, et al. Development and characterization of a clinical strain of Coxsackievirus A16 and an eGFP infectious clone. Virol Sin 2015;30:269–76.
[22] Li Z, Liu X, Wang S, Li J, Hou M, Liu G, et al. Identification of a nucleotide in 5' untranslated region contributing to virus replication and virulence of Coxsackievirus A16. Sci Rep 2016;6:20839.
[23] Wang X, Shen C, Chen T, Lan K, Huang Z, Zhang Y, et al. Improved plasmid-based recovery of coxsackievirus A16 infectious clone driven by human RNA polymerase I promoter. Virol Sin 2016;31:339–41.
[24] Yu R, Wang M, Liu L, Yan J, Fan J, Li X, et al. The development and characterization of a stable Coxsackievirus A16 infectious clone with Nanoluc reporter gene. Front Microbiol 2023;13:1101850.
[25] Yu R, Li X, Zhang P, Xu M, Zhao J, Yan J, et al. Integration of HiBiT into enteroviruses: A universal tool for advancing enterovirus virology research. Virol Sin 2024;39:422–33.
[26] Lauer KB, Borrow R, Blanchard TJ. Multivalent and Multipathogen Viral Vector Vaccines. Clin Vaccine Immunol 2017;24:e00298–316.
[27] Chou AH, Liu CC, Chang JY, Jiang R, Hsieh YC, Tsao A, et al. Formalin-inactivated EV71 vaccine candidate induced cross-neutralizing antibody against subgenotypes B1, B4, B5 and C4A in adult volunteers. PLoS One 2013;8:e79783.
[28] Liu CC, Chow YH, Chong P, Klein M. Prospect and challenges for the development of multivalent vaccines against hand, foot and mouth diseases. Vaccine 2014;32: 6177–82.
[29] Caine EA, Fuchs J, Das SC, Partidos CD, Osorio JE. Efficacy of a Trivalent Hand, Foot, and Mouth Disease Vaccine against Enterovirus 71 and Coxsackieviruses A16 and A6 in Mice. Viruses 2015;7(11):5919–32.
[30] Liu CC, Guo MS, Wu SR, Lin HY, Yang YT, Liu WC, et al. Immunological and biochemical characterizations of coxsackievirus A6 and A10 viral particles. Antiviral Res 2016;129:58–66.
[31] Zhang X, Zhang Y, Li H, Liu L. Hand-Foot-and-Mouth Disease-Associated Enterovirus and the Development of Multivalent HFMD Vaccines. Int J Mol Sci 2022;24:169.
[32] Shen YS, Chow YH, Fang CY, Wu SR, Chen CH, Huang MH, et al. The stability and immunogenicity of formalin-inactivated Enterovirus A71 whole virion vaccine after ten years of low temperature storage. J Microbiol Immunol Infect 2023;56: 1121–8.
[33] Domingo E, Sheldon J, Perales C. Viral quasispecies evolution. Microbiol Mol Biol Rev 2012;76:159–216.
[34] Sène MA, Kiesslich S, Djambazian H, Ragoussis J, Xia Y, Kamen AA. Haplotype-resolved de novo assembly of the Vero cell line genome. npj Vaccines 2021;6:106.
[35] Kiesslich S, Kamen AA. Vero cell upstream bioprocess development for the production of viral vectors and vaccines. Biotechnol Adv 2020;44:107608.
[36] Dumont J, Euwart D, Mei B, Estes S, Kshirsagar R. Human cell lines for biopharmaceutical manufacturing: history, status, and future perspectives. Crit Rev Biotechnol 2016;36:1110–2.
[37] Falsey AR, Sobieszczyk ME, Hirsch I, Sproule S, Robb ML, Corey L, et al. Phase 3 Safety and Efficacy of AZD1222 (ChAdOx1 nCoV-19) Covid-19 Vaccine. N Engl J Med 2021;385:2348–60.
[38] Wang L, Zhu M, Fang Y, Rong H, Gao L, Liao Q, et al. Bioinformatics-based prediction of conformational epitopes for Enterovirus A71 and Coxsackievirus A16. Sci Rep 2021;11:5701.
[39] Sun YS, Xia Y, Xu F, Lu HJ, Mao ZA, Gao M, et al. Development and evaluation of an inactivated coxsackievirus A16 vaccine in gerbils. Emerg Microbes Infect 2022; 11:1994–2006.
[40] Yi EJ, Kim YI, Song JH, Ko HJ, Ahn SH, Lee HJ, et al. Potential of a bivalent vaccine for broad protection against enterovirus 71 and coxsackie virus 16 infections causing hand, foot, and mouth disease. Vaccine 2023;41:6055–63.